Manipulations of oblique pulling affect sacroiliac joint displacements and ligament strains: a finite element analysis

Zhun Xu
Hengyang Medical College: University of South China
Ziyu Feng
Southern Medical University
Zhaocong Zhang
Southern Medical University
Liqing Liao
Southern Medical University
Dan Liu
Southern Medical University
Kunmu Zhang
Fujian University of Traditional Chinese Medicine
Yiguo Yan
University of South China Medical College
Yikai Li (lyk_doc@163.com)
Southern Medical University

Research Article

Keywords: Manipulations of oblique pulling, Sacroiliac joint, Displacement, Ligament strain, Finite element analysis

Posted Date: June 13th, 2022

DOI: https://doi.org/10.21203/rs.3.rs-1680881/v1

Abstract

Background

Clinical studies have found that Manipulation of oblique pulling (MOP) has a good clinical effect on sacroiliac joint (SIJ) pain without specific causes. However, there is no uniform standard for MOP at present. The effects of MOPs with different force points and directions on SIJs are not clear. The purpose of this study was to investigate the effects of four MOPs on the stresses and displacements of the normal SIJ and the strains of the surrounding ligaments.

Methods

A three-dimensional finite element model of the pelvis was established. Four MOPs were simulated. The stresses and displacements of the SIJ and the strains of the surrounding ligaments were analyzed under four MOPs.

Results

MOP-F2 caused the highest stress on the pelvis, at 85.0 MPa, while MOP-F3 caused the lowest stress on the pelvis, at 52.6 MPa. MOP-F3 produced the highest stress on the left SIJ, at 6.6 MPa, while MOP-F1 produced the lowest stress on the left SIJ, at 5.6 MPa. The four MOPs mainly produced anterior-posterior displacement of SIJ. The maximum value was 1.21 mm, produced by MOP-F2, while the minimal value was 0.96 mm, produced by MOP-F3. The four MOPs could all cause different degrees of ligament strain around the SIJ, and MOP-F2 produced the greatest ligament strain.

Conclusions

The four MOPs all produced small displacements of the SIJ and different degrees of ligament strain. MOP-F2 produced the largest displacement of SIJ and the greatest ligament strain, which could provide a certain reference for physiotherapists.

Background

Lower back pain usually caused by lumbar diseases, including myofasciitis, lumbar disc herniation and lumbar spondylolisthesis, is a common clinical symptom [1–3]. In recent years, it has been found that the lesion of sacroiliac joint (SIJ) can also cause lower back pain, accounting for 14.5%~22.5% [4]. The pathological mechanism is usually considered to be slight displacement of SIJ or the injury of surrounding ligaments and soft tissue caused by external forces or other factors. Clinically, it is called SIJ subluxation [5].

There are many treatment methods for SIJ subluxation, mainly including the following: (1)Take non-steroidal anti-inflammatory drugs（NSAID）and drugs for promoting blood circulation, so as to achieve the effects of anti-inflammatory, and promote blood circulation and remove blood stasis [6, 7]. (2) Inject glucocorticoids into the SIJ via a guide wire to produce a direct anti-inflammatory effect [8–10]. (3) Pull the subluxated SIJ back to normal position by manipulation to reduce nerve stimulation and relieve pain [11–14]. At present, the three methods have been applied in clinical treatment, and manipulation is the most widely used [15, 16].

Manipulation relieves the low back pain by changing mechanical environment of SIJ and surrounding tissue. This treatment method has little side effects, and can be easily accepted by patients. A large number of clinical studies have shown that Manipulation of oblique pulling (MOP) has a good effect on SIJ subluxation [17–19]. In our previous finite element study [20], we found that MOP could produce greater displacement and ligament strain of SIJ than manipulation of hip and knee flexion (MHKF) and lower limb hyperextension (MLLH). However, there is no uniform standard for MOP at present. Does MOP with different force points and directions produce different effects on the SIJ and its surrounding ligaments? None of these issues has been studied. Therefore, this study intends to establish a three-dimensional finite element model of pelvis and explore the effects of MOP on the stress and displacement of SIJ and strain of surrounding ligament by simulating four MOPs.

Methods

Model construction

A 3D finite element model of pelvis was established. Three-dimensional models of the sacrum and ilia were reconstructed from the computed tomography (CT) images of a healthy male volunteer (34 years old, 170 cm in height, and 65 kg in weight) using Mimics 20.0 (Materialise Company, Leuven, Belgium), and the cortical and cancellous regions of the bones were distinguished. Axial slices 0.5-mm thick spanning the entire pelvis were selected for model construction. All surface models were meshed using Geomagic 2013 (Raindrop Company, Marble Hill, USA). The SIJ was composed of cartilage and the end-plate of the sacrum and the ilia, with their surrounding ligaments. The cartilage was reconstructed with a uniform thickness. The regions of the articular surfaces were based on CT images, and the thicknesses of the cartilage were acquired from the literature. The sacral and iliac cartilages had thicknesses of 2 mm and 1 mm, respectively. The bone end-plate thicknesses of the sacral and iliac parts of the cartilage were assumed to be 0.23 mm and 0.36 mm, respectively. The gap between the two cartilages was set at 0.3 mm [21]. The material properties chosen from previous studies [21, 22] are summarized in Table 1.

The anterior sacroiliac ligament (ASL), short posterior sacroiliac ligament (SPSL), long posterior sacroiliac ligament (LPSL), sacrospinous ligament (SS), interosseous sacroiliac ligament (ISL), and sacrotuberous ligament (ST) complexes were modelled as 3D tension-only truss elements. The attachment regions were chosen according to the literature [21]. In total, the pelvic model contained 458,867 elements and 201,982 nodes. Fig. 1 shows the intact model with ligamentous attachments.

Simulation of MOPs

The simulation of MOP was as follows: The patient was in the right decubitus position. The right lower extremity was straight, and the left lower extremity was slightly bent. The therapist stood at the patient's ventral side. The therapist held the patient in position with one hand on the back of the scrum, the other hand on the anterior superior spine, pushing the ilium towards the back. Therefore, a large part of the sacrum and the right iliac crest were fixed. Then, a push force of 600 N along the ventral-dorsal direction was applied to the left anterior superior spine or anterior inferior iliac spine.

There were four MOPs. MOP-F1: The force was applied at the left anterior inferior iliac spine in a direction of 30° from the sagittal plane which roughly paralleled to the SIJ surface. MOP-F2: The force was applied at the left anterior inferior iliac spine, parallel to the sagittal plane. MOP-F3: The force was applied at the left anterior superior iliac spine in a direction of 30° from the SIJ surface. MOP-F4: The force was applied at the left anterior superior iliac spine, parallel to the sagittal plane. The detailed loading and boundary conditions, as well as the x-, y-, and z-axes, are described in Fig. 2. The compressive stresses and displacements of SIJ and the strains of ligaments for four MOPs were then investigated using Abaqus 2018 (Dassault Systemes S. A Company, Massachusetts, USA).

Mesh convergence study

In order to evaluate the degree of accuracy of pelvic model, mesh convergence study was carried out. Four mesh models were established according to different mesh fineness. The number of elements and nodes in each model are shown in Table 2. Following boundary conditions and material properties, loads, and constraints were described in detail in the above sections. MOP-F1, F2, F3 and F4 were applied to these meshes. Finally, the maximum stresses and displacements of the four models on the left SIJ surface of the sacrum under four MOPs were analyzed.

Model validation

Two studies were performed to validate this model. For the pelvic model, the distribution of the main strain of the pelvis was compared with that reported in the study of Zhang [23]. In our model, the distribution of the main strain of pelvis was analyzed under the single-legged stance. For the sacrum model, the relationship between displacement and load was compared with that indicated in cadaveric [24] and computational studies [21, 25]. When the bilateral ilia were fixed, five translational forces (anterior, posterior, superior, inferior, and mediolateral) of 294 N and three moments (flexion, extension, and axial rotation) of 42 Nm were applied to the centre of the sacrum, respectively. The displacements of a node lying in the mid-sagittal plane between the inferior S1 and superior S2 vertebral endplates were calculated. In this model, the displacements were investigated under the same loading.

Results

Mesh convergence study

The maximum stress and maximum displacement on the left SIJ surface of sacrum were analyzed for each of the meshes, under MOP-F1, F2, F3 and F4, which are shown in Fig. 3. The differences in maximum stress and maximum displacement between mesh 3 and mesh 4 under four MOPs were less than 5%, which was considered as reasonably close ranges. According to these results, mesh 3 with 458,867 elements was selected for further study.

Model validation

The stresses were located mainly in the upper and posterior areas of the acetabulum and extended to the iliac crest, the incisura ischiadica major, and the rear acetabulum. The area of stress concentration and maximum value of stress were consistent with those reported in a previous study [23]. Under eight loading conditions, the displacements were agreement not only with those in an experimental study but also with those in some computational studies [21, 24, 25], and these results are shown in Fig. 4.

Stress of pelvis and SIJ

The stress distributions of pelvis under four MOPs are shown in Fig. 5. Under MOP-F1, the stress of ventral pelvis was mainly concentrated on the left SIJ, extended to the arcuate line, the right SIJ, the right anterior inferior iliac spine, the upper part of right acetabulum, and the outer upper edge of right pubis. While the stress of dorsal pelvis was mainly concentrated around the left posterior inferior iliac spine and the greater ischial notch. The maximum stress value was 76.9 MPa. Under MOP-F2, the area of stress concentration was roughly the same as that under MOP-F1, but the maximum stress value was higher, at 85.0 MPa. Under MOP-F3, the stress of ventral pelvis was mainly concentrated on the left iliac crest, the left SIJ, the arcuate line, and the superior ramus of pubis, while the stress of dorsal pelvis was mainly concentrated on the left iliac crest and the greater sciatic notch. The maximum stress value was 52.6 MPa. Under MOP-F4, the area of stress concentration was roughly the same as that under MOP-F3. The maximum stress value was 80.0 MPa.

The distributions of stresses on the SIJ surface of sacrum are shown in Fig. 6. Under four MOPs, the principal stresses were concentrated on the anterior and inferior part of left SIJ. Higher stress was observed on the left SIJ for the four MOPs. Among them, MOP-F3 produced the highest stress on the left SIJ, at 6.6 MPa, while MOP-F1 produced the lowest stress on the left SIJ, at 5.6 MPa.

Displacement of SIJ

In MOP-F1, the displacements of the left SIJ were 1.088, 0.305 and 0.033 mm in the anterior-posterior (AP), superior-inferior (SI) and medial-lateral (MI) direction, respectively. In MOP-F2, the displacements were 1.211, 0.186 and 0.064 mm in the AP, SI and MI direction, respectively. In MOP-F3, the displacements were 0.962, 0.048 and 0.117 mm in the AP, SI and MI direction, respectively. In MOP-F4, the displacements were 1.105, 0.064 and 0.094 mm in the AP, SI and MI direction, respectively. The four MOPs mainly produced anterior-posterior displacement. The displacement of the left SIJ under four MOPs are shown in Fig. 7.

Strain of ligaments

The strains of six ligaments under four MOPs are shown in Fig. 8. For most of ligaments, the strain of the left ligament was greater than that of the right ligament under four MOPs. In MOP-F1, the left SS, ASL and ISL had a higher strain value, which were 3.71, 1.41 and 1.36%, respectively. In MOP-F2, the left SS, ST and ASL had a higher strain value, which were 4.29, 1.51 and 1.28%, respectively. In MOP-F3, the left SS, ASL and ST had higher strain value, which were 3.05, 1.61 and 1.09%, respectively. In MOP-F4, the left SS, SPSL and ASL had a higher strain value, which were 2.85, 1.90 and 1.04%, respectively.

Discussion

SIJ subluxation is a common clinical disease [26, 27]. The main cause of the disease is the minor displacement of SIJ or the injury of surrounding ligaments. According to many clinical reports [17, 28, 29], MOP could achieve good results in the treatment of SIJ subluxation. However, MOP has had no uniform standard for force point and direction. In this study, we established a three-dimensional finite element model of pelvis to explore the effects of MOP with different force points and directions on SIJ.

MOP-F1 and F2 were applied at the anterior inferior iliac spine, while MOP-F3 and F4 were applied at the anterior superior iliac spine. The force direction of F1 and F3 were roughly parallel to the SIJ surface, and the force direction of F2 and F4 were parallel to the sagittal plane of the pelvis. Anatomically, the anterior inferior iliac spine is located inside and below the anterior superior iliac spine, closer to the SIJ surface. Therefore, under the same direction of manipulation, MOP-F1 and F2 could produce greater maximum stress on the left hemi-pelvis than MOP-F3 and F4. In addition, since the anterior superior iliac spine was closer to the iliac crest region, MOP-F3 and F4 also caused greater stress on the left iliac crest region than MOP-F1 and F2. From the perspective of mechanical mechanism, the direction of manipulation parallel to the sagittal plane is more likely to produce greater stress on the left hemi-pelvis than that parallel to SIJ surface. What's more, the torque on the right hemi-pelvis was also greater, which could lead to greater stress on the right hemi-pelvis. Therefore, MOP-F2 and F4 produced greater stress on the left and right pelvis than MOP-F1 and F3.

The lower 1/3 part of SIJ is synovial joint, and the posterior and upper 1/3 part of SIJ is connected by interosseous ligaments [30], so the motion of SIJ is mainly undertaken by the lower 1/3 part of SIJ. The stresses on SIJ surfaces of sacra produced by four MOPs mainly distributed in the front and lower part of SIJ surfaces, which was related to the anatomical structure of SIJ. Due to the force point located on the left pelvis, the greater stresses were observed on the left SIJ surfaces under four MOPs. Compared with MOP-F2, MOP-F1 produced a smaller maximum stress on the left SIJ surface, which was connected to the direction of MOP-F1 parallel to SIJ surface. Compared with MOP-F4, MOP-F3 produced a greater maximum stress on the left SIJ surface. This phenomenon suggested that the SIJ surface was compressed and the motion forms of SIJ included translation and rotation.

The displacement of left SIJ was greater than that of right side under four MOPs. The displacement of left SIJ was 0.96 ~ 1.21 mm in AP direction, 0.03 ~ 0.12 mm in MI direction, and 0.05 ~ 0.31 mm in SI

direction. The values were all within 3 mm, which was consistent with previous research results [31, 32]. Under four MOPs, the displacement in AP direction was the largest in the three directions, which might be related to the fact that MOP could turn the pelvis outward. In AP direction, MOP-F2 and F4 produced the largest displacement of the left SIJ. The directions of forces applied by MOP-F2 and F4 were parallel to the sagittal plane, which was more likely to cause SIJ movement in AP direction than the directions of force parallel to the SIJ surface. In MI direction, MOP-F3 and F4 produced the largest displacements. The force points of the two manipulations were at the anterior superior iliac spine, which were far from the SIJ surface. Thus, the force arm was longer, which was easier to produce displacement in MI direction. The sacrum is broad at the top and narrow at the bottom. It is wedge-shaped and lies between the iliac bones on both sides forming SIJ [33]. This special structure makes the SIJ move up easily, but move down difficultly. The anterior inferior iliac spine is located inside and below the anterior superior iliac spine. Thus, MOP-F1 and F2 applied at the anterior inferior iliac spine could produce a larger upward displacement in SI direction.

Ligaments play an important role in maintaining pelvis stability. Abdelfattah et al. [34] found that the pubic symphysis and the anterior sacroiliac ligament played a key part in maintaining pelvis stability when the pelvis suffered "book-turning" violence. Sichting et al. [35] considered that the ligaments around SIJ not only played a role in maintaining mechanical stability of SIJ, but also acted as a neuromuscular feedback mechanism. Eichenseer et al. [25] through a finite element model, demonstrated that with the decrease of ligament stiffness, the stress and movement of SIJ would increase. Bohme et al. [36] found that the anterior sacroiliac ligament and the sacrotuberous ligament bore the largest load in the case of anterior and posterior compression fractures of pelvis, accounting for 80% and 17% of total load, respectively. The sacrospinous ligament played an important role in maintaining vertical stability of pelvis. Our results indicated that the strains of the sacrospinous ligament, the anterior sacroiliac ligament and the interosseous ligament were larger than the other three ligaments in most cases under four MOPs. Among them, the strain of sacrospinous ligament caused by MOP-F2 was the largest, at 4.29%. Under MOP-F2, the displacement of SIJ was the largest, which led to the largest ligament strain. The anterior sacroiliac ligament is a broad and thin ligament located in front of SIJ. The main displacement under four MOPs was in AP direction, so the anterior sacroiliac ligament would produce a greater strain.

In this study, there were four types of MOP. MOP-F2 and F4 produced the larger displacement in AP direction, at 1.21 and 1.11 mm, respectively. It showed that the manipulation parallel to the sagittal plane could cause a larger displacement. In addition, MOP-F2 and F4 also caused greater ligament strains. It could be seen that MOP-F2 and F4 are more effective manipulations to cause the displacement of SIJ and the strain of the surrounding ligaments.

There are some limitations in this study. First, the finite element model was established based on a single individual, while there are individual differences on age and gender for SIJ. Second, the ligaments in this model were built with linear materials, which had certain influence on reflecting the strain of ligaments. Third, this pelvic model only contained bones and ligaments. Soft tissues such as muscles and skin were not considered. Fourth, manipulations were analyzed based on a normal SIJ in this model, but

manipulations were applied to the subluxated SIJ clinically, so the results could not fully reflect the biomechanical characteristics of manipulations.

Conclusions

In this study, a three-dimensional finite element model of pelvis was established, and four manipulations with different force points and different directions were studied. The results showed that MOP-F3 and F4 caused greater stresses on the SIJ surface. The four MOPs all produced small displacements of the SIJ and different degrees of ligament strain. Among them, MOP-F2 and F4 could produce greater displacements of SIJ and ligament strains. MOP-F1 and F2 applied on the anterior inferior iliac spine mainly produced the displacement in AP and SI directions, while F3 and F4 applied on the anterior superior iliac spine mainly produced the displacement in AP and MI directions.

Abbreviations

SIJ
Sacroiliac joint
MOP
Manipulation of oblique pulling
ASL
Anterior sacroiliac ligament
ISL
Interosseous sacroiliac ligament
SS
Sacrospinous ligament
ST
Sacrotuberous ligament
LPSL
Long posterior sacroiliac ligament
SPSL
Short posterior sacroiliac ligament
AP
Anterior-posterior direction
SI
Superior-inferior direction
MI
Medial-lateral direction.

Declarations

Acknowledgements

Not applicable.

Authors' contributions

ZX, ZYFand ZCZ carried out the finite element analysis and drafted the manuscript. YKL, YGY and KMZ participated in the study design and discussion of the clinical results. DL and LQL constructed the finite element models, performed the biomechanical analysis. All of the authors read and approved the final manuscript.

Funding

This work was supported by the National Natural Science Foundation of China (grant number 81904316 and 81674095) and the Key Laboratory project of Orthopaedic Plant Research and Development of Hengyang City (grant number 2018KJ115). The funder mainly undertaken the design of the study and the analysis of the results, and was the corresponding author in this study.

Availability of data and materials

The datasets used and/or analyzed during the current study are available from the corresponding author upon reasonable request.

Ethics approval and consent to participate

The study was approved by Ethics Committee of the First Affiliated Hospital of University of South China. Written informed consent was available, and participant involved gave his consent for the use of individual data and experimental data.

Consent for publication

Not applicable.

Competing interests

The authors declare that they have no competing interests.

References

1. Minghelli B. Musculoskeletal spine pain in adolescents: Epidemiology of non-specific neck and low back pain and risk factors. J Orthop Sci. 2020;25(5):776–80.
2. Shmagel A, Foley R, Ibrahim H. Epidemiology of Chronic Low Back Pain in US Adults: Data From the 2009–2010 National Health and Nutrition Examination Survey. Arthritis Care Res. 2016;68(11):1688–94.
3. Swain CTV, Bradshaw EJ, Ekegren CL, Whyte DG. The Epidemiology of Low Back Pain and Injury in Dance: A Systematic Review. J Orthop Sports Phys Ther. 2019;49(4):239–52.

4. Lindsey DP, Perez-Orribo L, Rodriguez-Martinez N, Reyes PM, Newcomb A, Cable A, et al. Evaluation of a minimally invasive procedure for sacroiliac joint fusion-an in vitro biomechanical analysis of initial and cycled properties. Medical devices (Auckland, NZ). 2014;7:131–7.
5. Yang XW, Chen ZJ, Zhang SQ, Zhang MC, Li YK. A three-dimensional finite element analysis of sacroiliac joint exerted simulating oblique-pulling manipulation. J Pract Med. 2014;30(14):2228–30.
6. Ding YQ. MRI to evaluate the effect of Wenyang Bushen Decoction combined with Western medicine on sacroiliac joint lesions of ankylosing spondylitis. Chin J Traditional Med Sci Technol. 2020;27(1):87–9.
7. Min HK, Cho H, Park SH. Pilot study: non-steroidal anti-inflammatory drugs attenuate active inflammatory sacroiliac joint lesions in patients with early axial spondyloarthritis. Clin Exp Rheumatol. 2019;37(4):713.
8. Burnham T, Sampson J, Speckman RA, Conger A, Cushman DM, McCormick ZL. The Effectiveness of Platelet-Rich Plasma Injection for the Treatment of Suspected Sacroiliac Joint Complex Pain; a Systematic Review. Pain Med (Malden Mass). 2020;21(10):2518–28.
9. Dutta K, Dey S, Bhattacharyya P, Agarwal S, Dev P. Comparison of Efficacy of Lateral Branch Pulsed Radiofrequency Denervation and Intraarticular Depot Methylprednisolone Injection for Sacroiliac Joint Pain. Pain Physician. 2018;21(5):489–96.
10. Schneider BJ, Ehsanian R, Huynh L, Levin J, Zheng P, Kennedy DJ. Pain and Functional Outcomes After Sacroiliac Joint Injection with Anesthetic and Corticosteroid at Six Months, Stratified by Anesthetic Response and Physical Exam Maneuvers. Pain medicine (Malden. Mass). 2020;21(1):32–40.
11. Farazdaghi MR, Motealleh A, Abtahi F, Panjan A, Sarabon N, Ghaffarinejad F. Effect of sacroiliac manipulation on postural sway in quiet standing: a randomized controlled trial. Braz J Phys Ther. 2018;22(2):120–6.
12. Taber DJ, James GD, Jacon A. Manipulation under anesthesia for lumbopelvic pain: a retrospective review of 18 cases. J Chiropr Med. 2014;13(1):28–34.
13. Al-Subahi M, Alayat M, Alshehri MA, Helal O, Alhasan H, Alalawi A, et al. The effectiveness of physiotherapy interventions for sacroiliac joint dysfunction: a systematic review. J Phys therapy Sci. 2017;29(9):1689–94.
14. Zwirner J, Hammer N, Huang JN, He YF, Zhao XY, He ZT, et al. Treatment of sacroiliac joint dislocation by Zhuang medicine tendon therapy combined with chiropractic manipulation. Sci Rep. 2019;32(9):806–9.
15. Li CH, Tang LZ. Literature evaluation on the randomized controlled trials of orthopedic therapy in treating of staggered sacroiliac joints. Clin J traditional Chin Med. 2017;29(07):1031–5.
16. Yang WS. Clinical observation on the treatment of staggered sacroiliac joint by manipulation of pulling and stretching. J practical traditional Chin Med. 2016;32(11):1123–4.
17. Yang YZ, Gan YJ, Zheng ZZ. Clinical observation on the treatment of staggered sacroiliac joint by massage and manipulation of modified oblique pulling. Chin Manipulation Rehabilitation Med.

2018;9(15):12–4.
18. Chen H, Zeng KX, Gai JJ. 33 cases of staggered sacroiliac joint treated by manipulation of modified oblique pulling. Chin Manipulation & Qi Gong therapy. 2007;23(01):41–2.
19. Bao XR, Wang Q, Peng L, Yu Z. Modified inclined pulling manipulation in treatment of disorders of sacroiliac joint. Chin Gen Pract. 2013;16(3):310–1.
20. Xu Z, Li Y, Zhang S, Liao L, Wu K, Feng Z, et al. A finite element analysis of sacroiliac joint displacements and ligament strains in response to three manipulations. BMC Musculoskelet Disord. 2020;21(1):709.
21. Kim YH, Yao Z, Kim K, Park WM. Quantitative investigation of ligament strains during physical tests for sacroiliac joint pain using finite element analysis. Man Ther. 2014;19(3):235–41.
22. Lee CH, Hsu CC, Huang PY. Biomechanical study of different fixation techniques for the treatment of sacroiliac joint injuries using finite element analyses and biomechanical tests. Comput Biol Med. 2017;87:250–7.
23. Zhang QH, Wang JY, Lupton C, Heaton-Adegbile P, Guo ZX, Liu Q, et al. A subject-specific pelvic bone model and its application to cemented acetabular replacements. J Biomech. 2010;43(14):2722–7.
24. Miller JA, Schultz AB, Andersson GB. Load-displacement behavior of sacroiliac joints. J Orthop Res. 1987;5(1):92–101.
25. Eichenseer PH, Sybert DR, Cotton JR. A finite element analysis of sacroiliac joint ligaments in response to different loading conditions. Spine. 2011;36(22):e1446-52.
26. Lei YK, Fan BH. Advances in anatomical and biomechanical mechanisms of manipulation for sacroiliac joint subluxation. J Traditional Chin Orthop Traumatol. 2011;23(01):40–2.
27. Zhang SQ, Li NQ, Qi J, Li YK. Historical evolution of sacroiliac joint malposition based on bibliometric analysis. Chin J Tissue Eng Res. 2018;22(27):4316–21.
28. Zhang CC, Chang MM, Yuan X, Tang SJ. Research progress of manipulation of oblique pulling for lumbar spine. J Traditional Chin Orthop Traumatol. 2020;32(5):22–5.
29. Zhou SC, Cheng HH. Application of manipulation of oblique pulling and lower limb hyperextension in the treatment of posterior sacroiliac joint subluxation. Chin Manipulation&Rehabilitation Med. 2011;02(2):85–6.
30. Zhang YQ, Liu W, Fu XY, Li YK. The radiological anatomic observations of sacroiliac joint. Chin J Clin Anat. 2009;27(01):73–5.
31. Walker JM. The sacroiliac joint: a critical review. Phys Ther. 1992;72(12):903–16.
32. Wilke HJ, Fischer K, Jeanneret B, Claes L, Magerl F. In vivo measurement of 3-dimensional movement of the iliosacral joint. Z Orthop Ihre Grenzgeb. 1997;135(6):550–6.
33. Shi D, Wang F, Wang D, Li X, Wang Q. 3-D finite element analysis of the influence of synovial condition in sacroiliac joint on the load transmission in human pelvic system. Med Eng Phys. 2014;36(6):745–53.

34. Abdelfattah A, Moed BR. Ligamentous contributions to pelvic stability in a rotationally unstable open-book injury: a cadaver study. Injury. 2014;45(10):1599–603.
35. Sichting F, Rossol J, Soisson O, Klima S, Milani T, Hammer N. Pelvic belt effects on sacroiliac joint ligaments: a computational approach to understand therapeutic effects of pelvic belts. Pain Physician. 2014;17(1):43–51.
36. Bohme J, Lingslebe U, Steinke H, Werner M, Slowik V, Josten C, et al. The extent of ligament injury and its influence on pelvic stability following type II anteroposterior compression pelvic injuries-A computer study to gain insight into open book trauma. J Orthop Res. 2014;32(7):873–9.

Tables

Table 1
Material properties of the sacrum, ilium, pubic symphysis and endplate.

		Young' s modulus (MPa)	Poisson' s ratio
Sacrum	Cortical	12,000	0.3
	Cancellous	100	0.2
Ilium	Cortical	12,000	0.3
	Cancellous	100	0.2
Pubic symphysis		5	0.45
Articular cartilage		100	0.3
Endplate		1000	0.4

Table 2
Element and node numbers for four different mesh resolutions.

	Element number	Node number
Mesh 1	142,007	58,480
Mesh 2	243,492	101,724
Mesh 3	458,867	201,982
Mesh 4	1,051,834	481,435

Figures

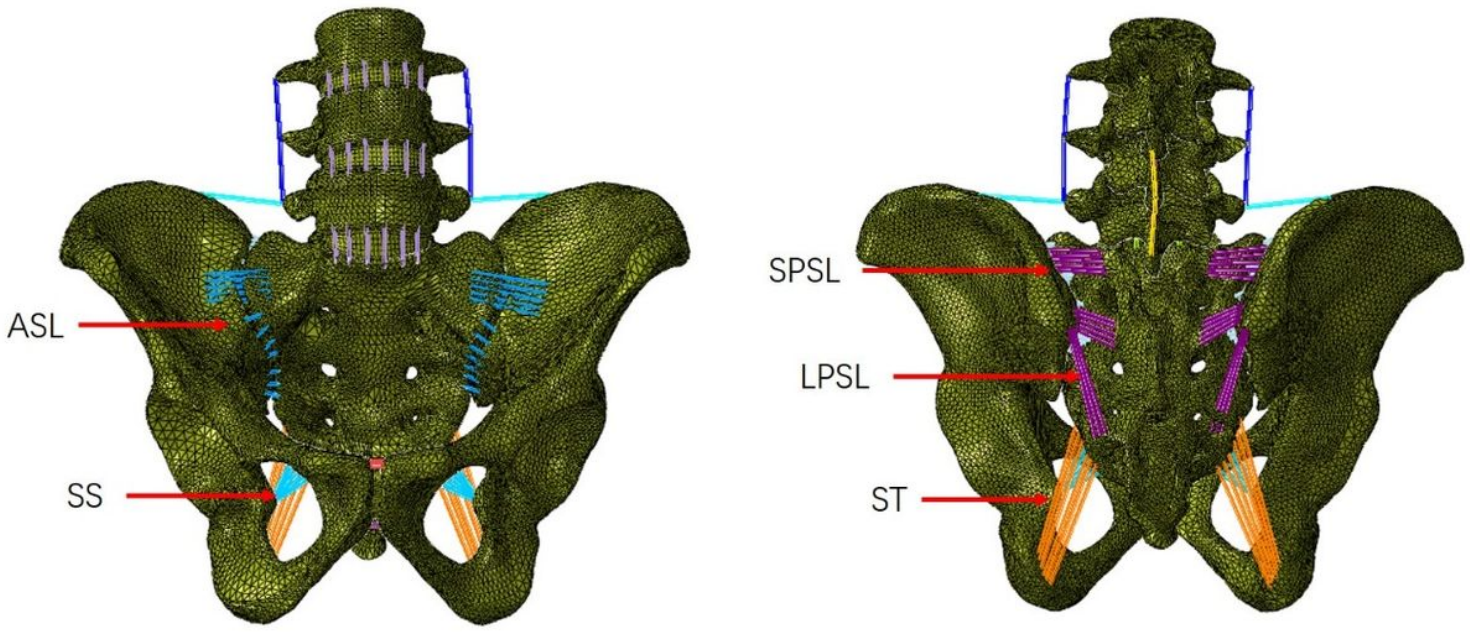

Figure 1

Ventral (left) and Dorsal (right) views of the finite element model. Ligaments are represented in color lines, with red arrows identifying each ligament complex (note the interosseous sacroiliac ligament is not visible in anterior-posterior views). ASL indicates anterior sacroiliac ligament; LPSL, long posterior sacroiliac ligament; SPSL, short posterior sacroiliac ligament; SS, sacrospinous ligament; ST, sacrotuberous ligament

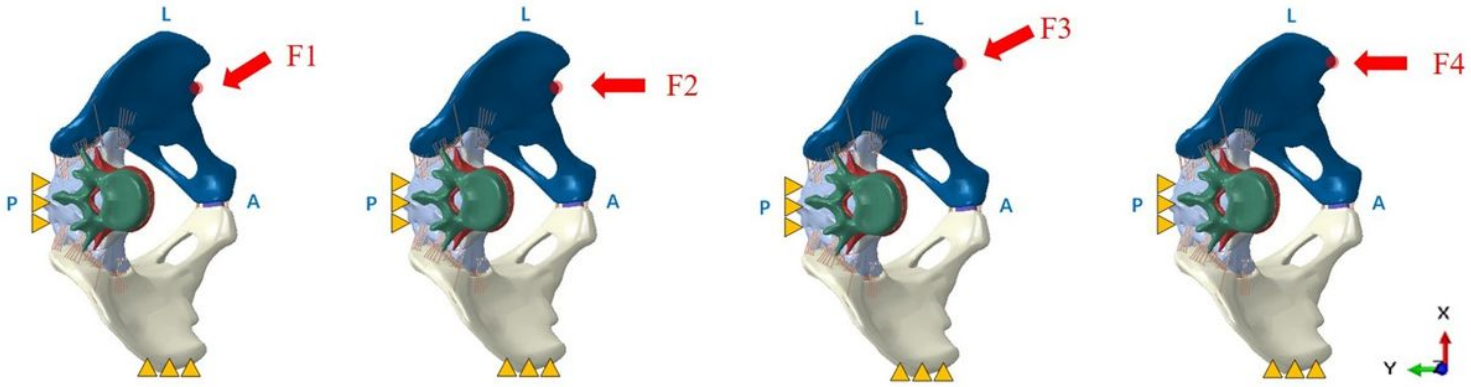

Figure 2

Loading and boundary conditions for four manipulations of oblique pulling. The yellow triangles represent the fixed sites of pelvic model. **a** Manipulation of oblique pulling-F1; **b** Manipulation of oblique pulling-F2; **c** Manipulation of oblique pulling-F3; **d** Manipulation of oblique pulling-F4.

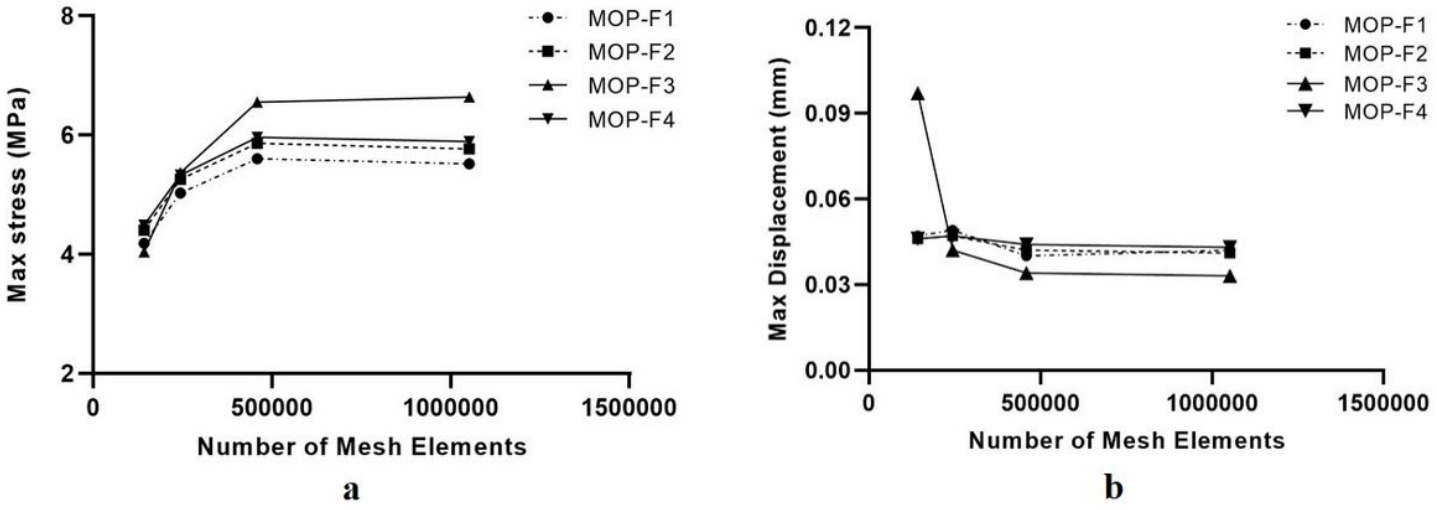

Figure 3

a Maximum stresses on the left SIJ surface of sacrum for different number of mesh elements, under MOP-F1, F2, F3 and F4. **b** Maximum displacements on the left SIJ surface of sacrum for different number of mesh elements, under MOP-F1, F2, F3 and F4.

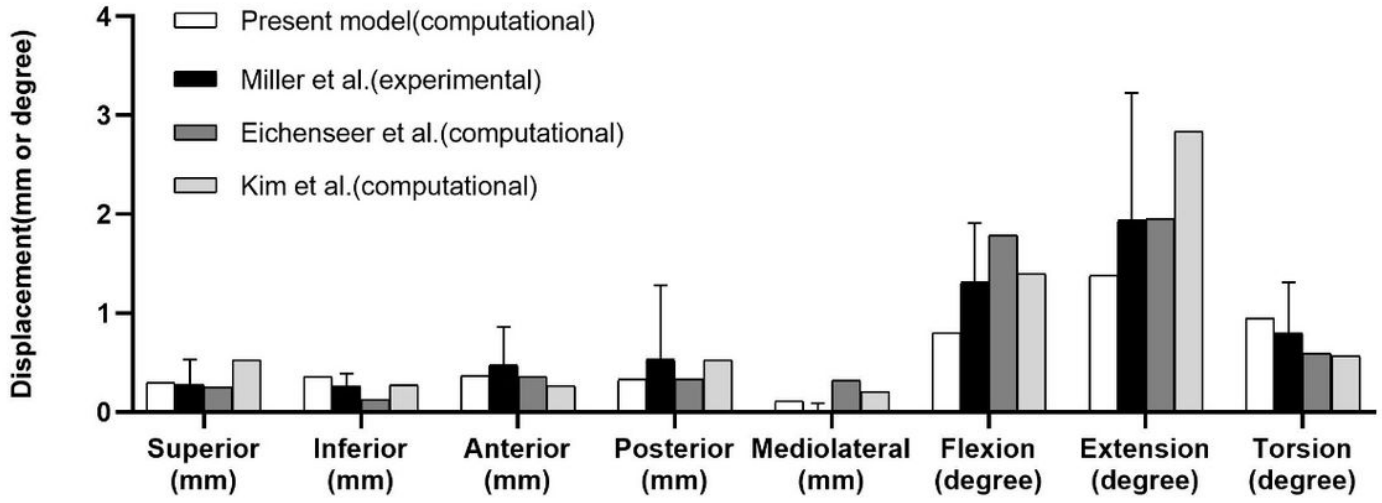

Figure 4

Comparison of sacral displacements under eight loadings comparable to those in previous experimental and computational studies.

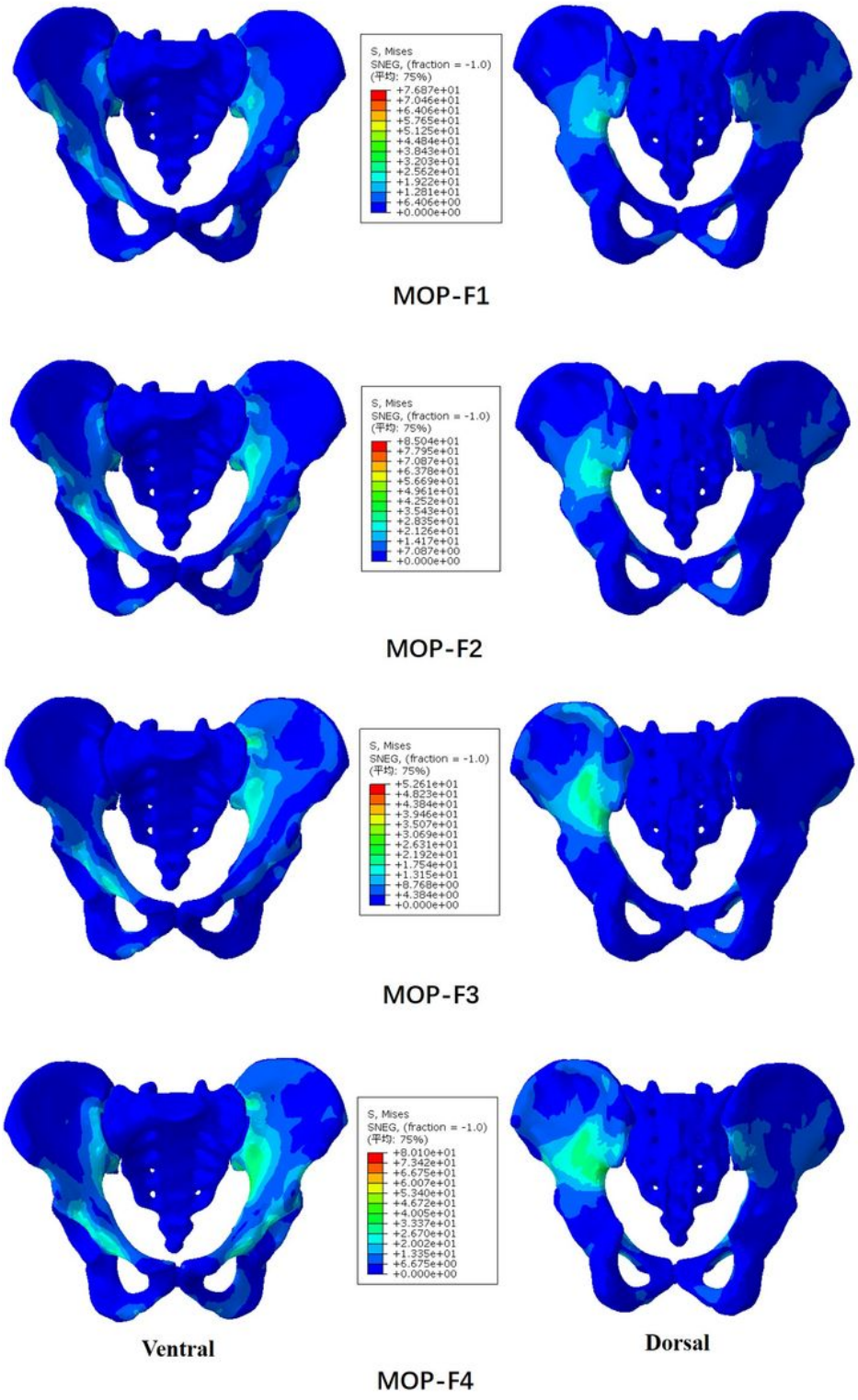

Figure 5

Distribution of compressive stresses on the cortical bone of pelvis under MOP-F1, F2, F3 and F4.

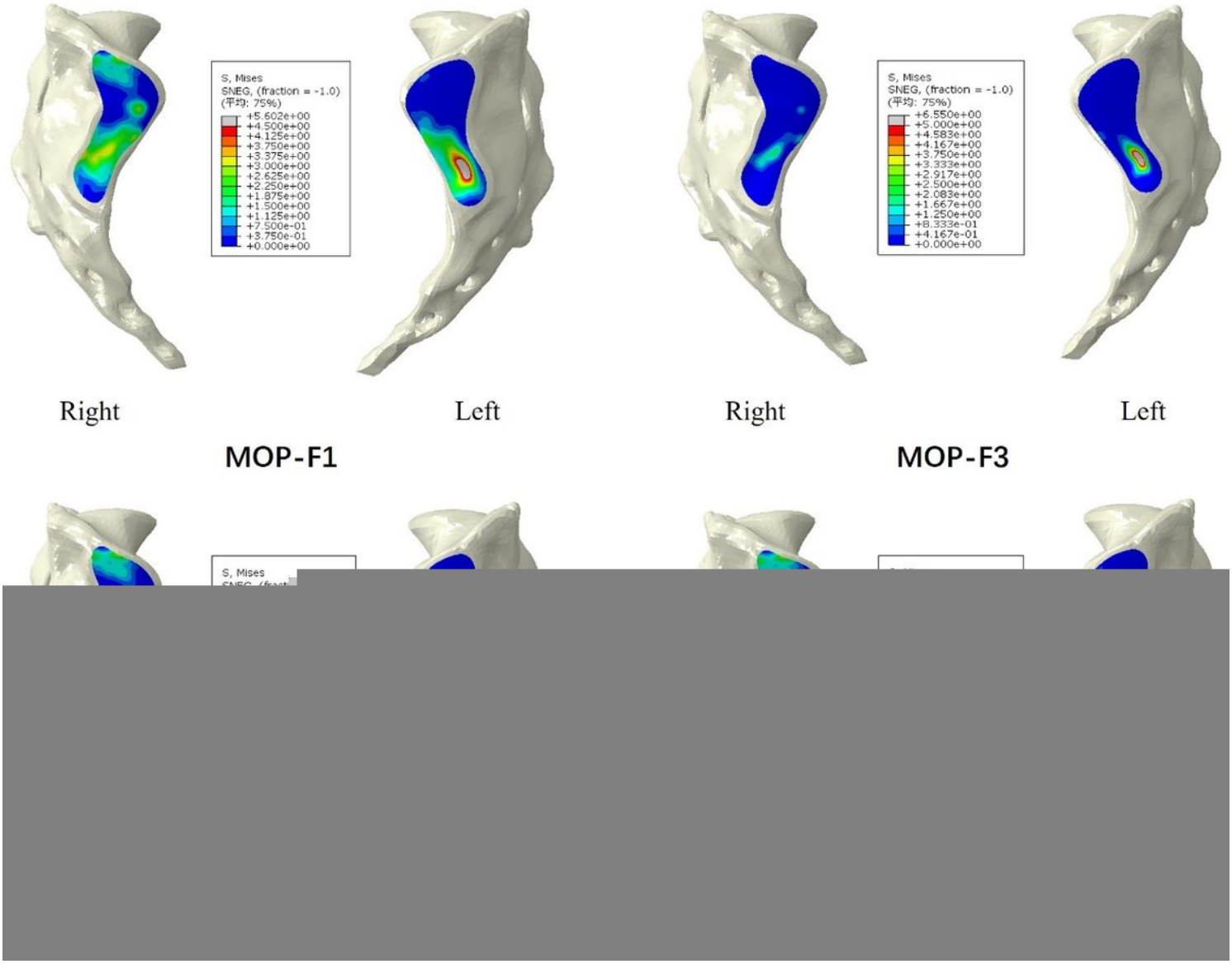

Figure 6

Distribution of compressive stresses on the SIJ surface of sacrum under MOP-F1, F2, F3 and F4.

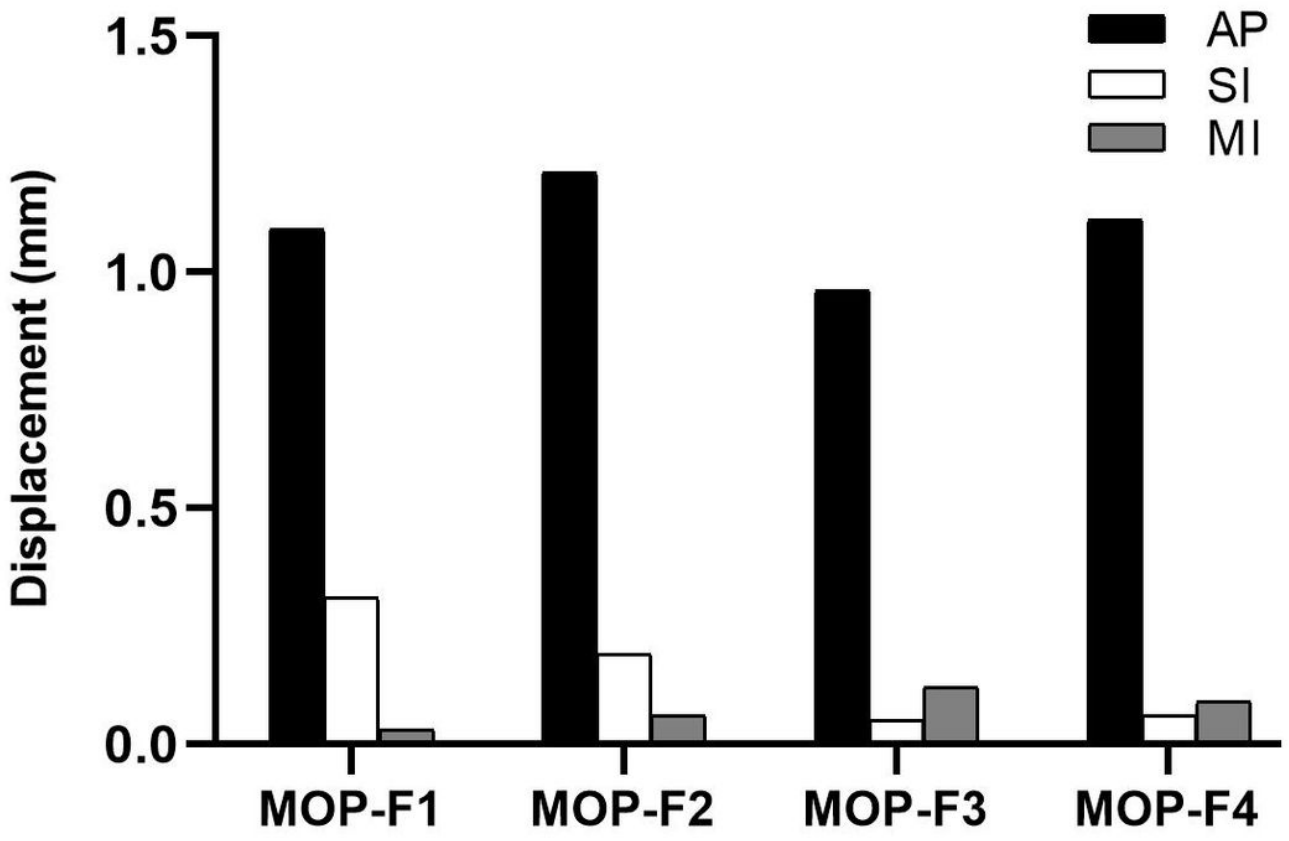

Figure 7

The displacements of left SIJ under MOP-F1, F2, F3 and F4. AP: Anterior-posterior direction; SI: Superior-inferior direction; MI: Medial-lateral direction

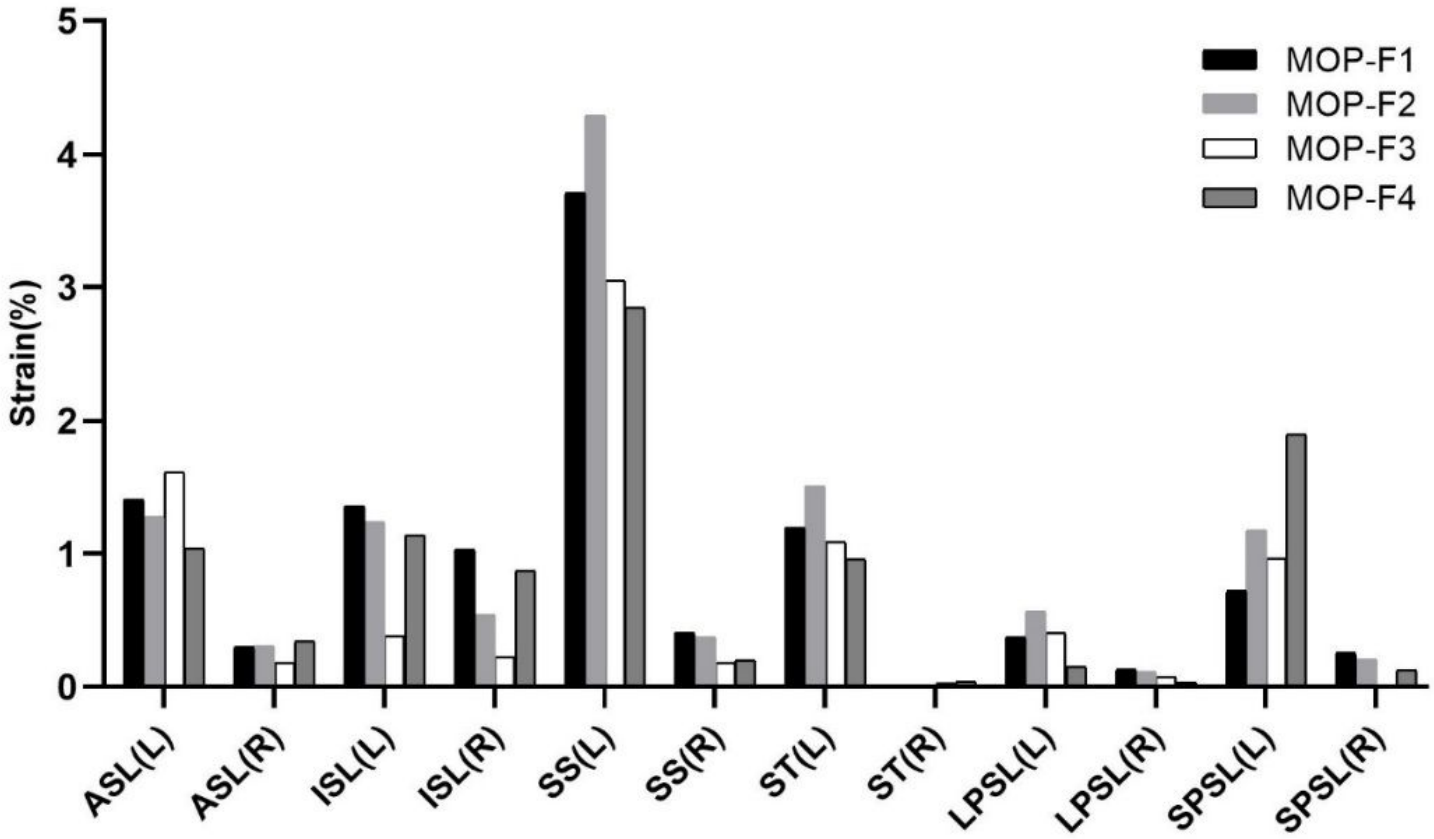

Figure 8

Ligament strains under MOP-F1, F2, F3 and F4. L: Left; R: Right; ASL: Anterior sacroiliac ligament; ISL: Interosseous sacroiliac ligament; SS: Sacrospinous ligament; ST: Sacrotuberous ligament; LPSL: long posterior sacroiliac ligament; SPSL: Short posterior sacroiliac ligament